



Published in final edited form as:

*Biomed Mater.* 2008 June ; 3(2): 025012. doi:10.1088/1748-6041/3/2/025012.

## Preparation and evaluation of a high-strength biocompatible glass-ionomer cement for improved dental restoratives

D Xie<sup>1</sup>, J Zhao<sup>1</sup>, Y Yang<sup>2</sup>, J Park<sup>1</sup>, T M Chu<sup>1</sup>, J T Zhang<sup>2</sup>

<sup>1</sup>Department of Biomedical Engineering, Purdue School of Engineering and Technology, Indiana University–Purdue University at Indianapolis, Indianapolis, IN 46202, USA

<sup>2</sup>Department of Pharmacology, School of Medicine, Indiana University, Indianapolis, IN 46202, USA

### Abstract

We have developed a high-strength light-cured glass-ionomer cement (LCGIC). The polymer in the cement was composed of the 6-arm star-shape poly(acrylic acid) (PAA), which was synthesized using atom-transfer radical polymerization. The polymer was used to formulate with water and Fuji II LC filler to form LCGIC. Compressive strength (CS) was used as a screening tool for evaluation. Commercial glass-ionomer cement Fuji II LC was used as control. The results show that the 6-arm PAA polymer exhibited a lower viscosity in water as compared to its linear counterpart that was synthesized via conventional free-radical polymerization. This new LCGIC system was 48% in CS, 77% in diametral tensile strength, 95% in flexural strength and 59% in fracture toughness higher but 93.6% in shrinkage lower than Fuji II LC. An increasing polymer content significantly increased CS, whereas an increasing glass filler content increased neither yield strength nor ultimate CS except for modulus. During aging, the experimental cement showed a significant and continuous increase in yield strength, modulus and ultimate CS, but Fuji II LC only showed a significant increase in strength within 24 h. The experimental cement was very biocompatible *in vivo* to bone and showed little *in vitro* cytotoxicity. It appears that this novel LCGIC cement will be a better dental restorative because it demonstrated significantly improved mechanical strengths and better *in vitro* and *in vivo* biocompatibilities as compared to the current commercial LCGIC system.

### Introduction

Glass-ionomer cements (GICs), one of the most promising materials among current dental restoratives, have been successfully applied in dentistry for more than 27 years [1–4]. The success of these cements is attributed to the facts that they have unique properties such as direct adhesion to tooth structure and base metals [5, 6], anticariogenic properties due to release of fluoride [7], thermal compatibility with tooth enamel and dentin because of low coefficients of thermal expansion similar to those of the tooth structure [8], minimized microleakage at the tooth–enamel interface due to low shrinkage [8] and low cytotoxicity [9, 10].

The setting and adhesion mechanism of GICs can be simply described as an acid–base reaction between calcium and/or aluminum cations released from a reactive glass and carboxyl anions pendent on polyacid [2, 11]. The polymer backbones of GICs have been made by poly(acrylic acid) homopolymer, poly(acrylic acid-co-itaconic acid) or/and poly(acrylic acid-co-maleic acid) copolymers [1, 2, 11]. These GICs are called conventional glass-ionomer cements (CGICs) [1–4]. Despite numerous advantages of CGIC, brittleness and low tensile and flexural strengths have limited the current CGIC for use only at certain low stress-bearing sites such as Class III and Class V cavities [1, 2]. Much effort has been made to improve the mechanical strengths of CGIC [1, 4, 11], and the focus has been mainly on the improvement of the polymer backbone or matrix [1, 4, 11, 12–18]. Briefly, two main strategies have been applied. One is to incorporate hydrophobic pendent (meth)acrylate moieties onto the polyacid backbone in CGIC to make it become light- or redox-initiated resin-modified GIC (RMGIC) [12–15, 17] and the other is to directly increase the molecular weight (MW) of the polyacid [16–18]. As a result, the former has shown significantly improved tensile and flexural strengths as well as handling properties [12–15, 17]. The strategy of increasing MW of the polyacid by introducing either amino acid derivatives or N-vinylpyrrolidone has also shown enhanced mechanical strengths [16–18]; however, the working properties were somehow decreased because strong chain entanglements formed in these high MW linear polyacids resulted in an increased solution viscosity [16, 17]. So far, all the polyacids used in GIC formulations have been linear polymers and synthesized via conventional free-radical polymerization.

It has been noted that polymers with star, hyperbranched or dendritic shapes often demonstrate a low solution or melt viscosity because these molecular structures behave similar to a solution of hard spheres and exhibit limited chain entanglements, which is beneficial to polymer processing [19, 20]. Therefore, we hypothesized that it might be possible to increase MW without or with less viscosity increase if the polyacids in current CGIC were star-shaped (spherical) or dendritic. As we know, however, it is absolutely impossible to make the polyacids with such molecular architectures by using current conventional free-radical polymerization techniques. Nevertheless, the most recent development of living free-radical polymerization technologies such as atom-transfer radical polymerization (ATRP) [21] may well help us to test our proposed hypothesis.

Although light-cured RMGICs (LCGIC) have demonstrated reduced moisture sensitivity, improved mechanical strengths, extended working time and ease of clinical handling [1, 4], there have been concerns regarding their biocompatibility [9, 10]. It has been found that LCGIC are less biocompatible than CGIC [22, 23]. The reason is attributed to 2-hydroxyethyl methacrylate (HEMA) and other low molecular weight species such as additives and co-initiators in LCGIC formulations [22]. HEMA is incorporated as the major and necessary component in LCGIC formulations for enhancing water solubility of the methacrylate-containing polyacids because HEMA bears both hydroxyl and methacrylate groups. So far, almost all the commercially available LCGIC contain HEMA [1, 4, 22]. Free HEMA leached from LCGIC such as Vitremer has been reported to exhibit cytotoxicity when it contacts the dental pulp tissue and osteoblasts [24, 25]. Theoretically speaking, almost all the low molecular weight molecules are cytotoxic to the cells or tissues more or less [26]. That is why CGIC show little cytotoxicity to dental pulp or the other tissues

[22, 23]. However, as we know, by using current technologies it is almost impossible to formulate a LCGIC without incorporating any low MW amphiphilic molecules like HEMA. In this paper, we also hypothesized to tether amphiphilic methacrylate functionality onto the proposed polyalkenoic acid in order to substitute very hydrophobic methacrylate moieties currently being used in LCGIC [1, 4] and thus to eliminate HEMA, which may provide a promising route for formulating a very biocompatible LCGIC for improved dental and orthopedic applications.

The objective of this study was to synthesize and characterize novel 6-arm PAA via the ATRP technique, tether *in situ* light-curable amphiphilic methacrylate functionality onto the polyacid backbone, use this light-curable PAA to formulate a high-strength LCGIC and evaluate the mechanical strengths and *in vitro* cytotoxicity as well as *in vivo* bone compatibility of the formed cements.

## Materials and methods

### Materials

Dipentaerythritol, triethylamine (TEA), 2-bromoisobutyryl bromide (BIBB), CuBr, N,N,N',N',N''-pentamethyldiethylenetriamine (PMDETA), dl-camphoroquinone (CQ), 2-(dimethylamino)ethyl methacrylate (DMAEMA), 2,2'-azobisisobutyronitrile (AIBN), pyridine, tert-butyl acrylate (t-BA), glycidyl methacrylate (GM), anhydrous magnesium sulfate (MgSO<sub>4</sub>), sodium hydroxide (NaOH), hydrochloric acid (HCl, 37%), diethyl ether, N,N-dimethylformamide (DMF), tetrahydrofuran (THF), deuterated methyl sulfoxide and ethyl acetate were used as received from VWR International Inc (Bristol, CT) without further purifications. Light-cured Fuji II LC kit and Fuji II LC glass powders were supplied by GC America Inc (Alsip, IL).

### Synthesis and characterization

**Synthesis of the 6-arm initiator.**—The 6-arm initiator was synthesized following the procedures described by Wang *et al.*, with a slight modification [27]. Briefly, to a reactor charged with 100 ml of TEA, 15 g of dipentaerythritol and 200 ml of THF, a mixture of 100 ml of BIBB in 25 ml of THF was added dropwise by stirring at room temperature. After the addition was completed, an additional 1 h was allowed to complete the reaction. The solution was washed with 5% NaOH and 1% HCl and then extracted with ethyl acetate. The extract was dried with anhydrous MgSO<sub>4</sub>, concentrated *in vacuo* and crystallized. The final product was recrystallized from diethyl ether. The schematic diagram for the 6-arm initiator synthesis is shown in figure 1(a).

**Synthesis of the 6-arm PAA via ATRP.**—To a flask containing dioxane (10.0 g), a mixture of 6-arm initiator (1% by mole), PMDETA (3%, ligand) and t-BA (10.0 g) was charged. CuBr (3%) was incorporated under N<sub>2</sub> purging after the above solution was degassed and nitrogen-purged via three freeze–thaw cycles. The solution was then heated to 120 °C to initiate ATRP [28]. Fourier transform infrared (FT-IR) spectroscopy was used to monitor the reaction. After the polymerization was completed, the poly(t-BA) polymer was precipitated from water. CuBr and PMDETA were removed by re-precipitation from

dioxane/water. The colorless poly(t-BA) polymer was then hydrolyzed in a mixed solvent of dioxane and HCl (37%) [29] (dioxane/HCl = 1/3) under a refluxed condition for 24 h. The formed PAA was dialyzed against water until the pH became neutral. The purified 6-arm PAA was obtained upon freeze-drying. The reaction scheme for the polymer synthesis via ATRP is described in figure 1(b).

**Synthesis of the linear PAA via conventional free-radical polymerization.—**

Linear PAA was synthesized following our previous publication [30]. Briefly, to a flask containing AIBN and THF, a mixture of AA and THF was added dropwise. Under a nitrogen blanket, the reaction was initiated and run at 62 °C for 10 h. The polymer was purified by precipitation using ether and drying in a vacuum oven.

**Synthesis of the GM-tethered 6-arm PAA.—**Typically, to a three-neck flask containing the 6-arm PAA (8.2 g), THF (36 ml) and BHT (1%, by weight), a mixture of GM (7.2 g), THF (21 ml) and pyridine (1% of GM, by weight) was added dropwise. Under a nitrogen blanket, the reaction was initiated and run at 60 °C for 5 h and then kept at room temperature overnight. FT-IR spectroscopy was used to monitor the reaction. The polymer tethered with GM was recovered by precipitation from diethyl ether, followed by drying in a vacuum oven at 23 °C. The yield was greater than 95%. The scheme for synthesis of the GM-tethered 6-arm PAA is described in figure 1(c).

**Characterization of the 6-arm initiator and polymers.—**The synthesized 6-arm initiator was characterized by melting point identification, FT-IR spectroscopy and nuclear magnetic resonance (NMR) spectroscopy. The polymers were characterized by FT-IR, NMR and vapor pressure osmometry (VPO). The GM-tethered polymers were identified by FT-IR and NMR spectroscopy. The melting point of the initiator was measured using a digital melting point apparatus (Electrothermal IA 9000 Series, Electrothermal Engineering Ltd, Essex, UK). FT-IR spectra were obtained on a FT-IR spectrometer (Mattson Research Series FT/IR 1000, Madison, WI). <sup>1</sup>H NMR spectra were obtained on an ARX-300 NMR spectrometer using deuterated methyl sulfoxide as a solvent. The MW of the linear poly(acrylic acid) was determined in DMF using a vapor pressure osmometer (K-7000, ICON Scientific, Inc., North Potomac, MD). The MW of the 6-arm poly(acrylic acid) was determined by the <sup>1</sup>H NMR spectrum.

The viscosities of the liquid formulated with the GM-tethered 6-arm PAA and distilled water in different weight ratios were determined at 23 °C using a programmable cone/plate viscometer (RVDV-II + CP, Brookfield Eng. Lab. Inc., Middleboro, MA).

## Evaluations

**Formulation and preparation of specimens for strength tests.—**The cements were formulated with a two-component system (liquid and powder) [17]. The liquid was formulated with the GM-tethered polymer, water, 0.7% CQ (photo-initiator, by weight), 1.4% DC (activator) and 0.05% HQ (stabilizer). Fuji II LC glass powder was used to formulate the cements with a powder/liquid (P/L) ratio of 2.7. Fuji II LC kit with a P/L ratio

of 3.2, where the P/L ratio was applied as recommended by the manufacturer, was used as control.

Specimens were fabricated at room temperature according to the published protocol [16, 17, 31]. Briefly, the cylindrical specimens were prepared in glass tubing with dimensions of 4 mm in diameter by 8 mm in length for compressive strength (CS) and 4 mm in diameter by 2 mm in length for diametral tensile strength (DTS) tests. The rectangular specimens were prepared in split Teflon molds with dimensions of 3 mm in width  $\times$  3 mm in thickness  $\times$  25 mm in length for flexural strength (FS) and 4 mm in width  $\times$  2 mm in thickness  $\times$  20 mm in length, fitted with a sharp blade for generating a 2 mm long notch, for fracture toughness (FT) tests [31]. A transparent plastic window was used on the top of the split mold for light exposure. Specimens were exposed to blue light (EXAKT 520 Blue Light Polymerization Unit, 9W/71, GmbH, Germany) for 1 min, followed by conditioning in 100% humidity for 15 min, then removed from the mold and conditioned in distilled water at 37 °C for 24 h unless specified, prior to testing.

**Strength measurements.**—Testing of specimens was performed on a screw-driven mechanical tester (QTest QT/10, MTS Systems Corp., Eden Prairie, MN), with a crosshead speed of 1 mm min<sup>-1</sup> for CS, DTS, FS and FT measurements. The FS and FT tests were performed in three-point bending, with a span of 20 mm and 16 mm, respectively, between supports. The sample sizes were  $n = 6-8$  for each test.

CS was calculated using the equation  $CS = P/\pi r^2$ , where  $P$  = the load at fracture and  $r$  = the radius of the cylinder. DTS was determined from the relationship  $DTS = 2P/\pi dt$ , where  $P$  = the load at fracture,  $d$  = the diameter of the cylinder and  $t$  = the thickness of the cylinder. FS was obtained using the expression  $FS = 3Pl/2bd^2$ , where  $P$  = the load at fracture,  $l$  = the distance between the two supports,  $b$  = the breadth of the specimen and  $d$  = the depth of the specimen. FT [31] was calculated using the equations  $K_{IC} = [(PS)/(BW^{1.5})] [f(a/W)]$  and  $f(a/W) = 3(a/W)^{0.5} [1.99 - (a/W)(1 - a/W)(2.15 + 3.93a/W + 2.7a^2/W^2)]/2(1 + 2a/W)(1 - a/W)^{1.5}$ , where  $K_{IC}$  = fracture toughness,  $P$  = load at fracture,  $S$  = span between supports,  $B$  = specimen thickness,  $W$  = specimen width and  $a$  = crack length ( $W/2$ ).

**Determination of polymerization shrinkage.**—The polymerization shrinkage of the cement was determined using the equation  $\% \text{shrinkage} = (1 - d_{\text{uncured}}/d_{\text{cured}}) \times 100$ , where  $d_{\text{cured}}$  = density of the cured cement and  $d_{\text{uncured}}$  = density of the uncured cement [32]. The densities of the uncured and cured cements were respectively determined by weighing the cement paste, injected from a calibrated syringe, and weighing the cured cylindrical specimens, whose volumes were measured in a calibrated buret in the presence of hexane. The mean values were averaged from three readings.

## Biocompatibility test

**In vitro cytotoxicity test using an MTT assay.**—The experimental light-cured cement (EXPLC) and Fuji II LC were used for *in vitro* cytotoxicity study. A plain cell culture medium was used as negative control (NC). Specimens with dimensions of 4 mm in diameter by 2 mm in thickness [22] were fabricated similar to the method described above. Immediately after being light-cured, each cured specimen was quickly rinsed with a 70%

ethanol and phosphate buffer saline (PBS) solution, followed by soaking in a 500  $\mu\text{l}$  cell culture medium in a 48-well plate in a humidified incubator at 37 °C with 5% CO<sub>2</sub> and 95% air for 7 days, for preparation of eluates. The surface area to volume ratio was 1 cm<sup>2</sup> ml<sup>-1</sup>, which was set according to the ISO standards (0.5–6.0 cm<sup>2</sup> ml<sup>-1</sup>) [33]. Five specimens of each material ( $n = 5$ ) were prepared and used for statistical analysis.

The methyltetrazolium (MTT) test was performed as described previously [34]. Briefly, Balb/c 3T3 mouse fibroblast cells were plated in a 96-well plate at  $2 \times 10^3$  cells per well in 50  $\mu\text{l}$  of Dulbecco's Modified Eagle Media (DMEM) supplemented with 10% donor calf serum (DCS), 100 U ml<sup>-1</sup> penicillin and 100  $\mu\text{g}$  ml<sup>-1</sup> streptomycin. After incubation at 37 °C overnight, the medium was replaced with 100  $\mu\text{l}$  of the fresh medium containing different concentrations of eluate (0, 5, 10, 20, 40 and 80%). The cells were then incubated for 3 days before MTT testing. The MTT test was conducted by adding 10  $\mu\text{l}$  of MTT (5 mg ml<sup>-1</sup>) into a well to a final concentration of 0.5 mg ml<sup>-1</sup> and then incubating the plate at 37 °C for another 2 h. An equal volume (100  $\mu\text{L}$ ) of a solubilization solution (10% SDS in 0.01 M HCl) was then added to the plate followed by incubating the plate at 37 °C overnight. The optical density (OD<sub>570</sub>) was measured at 570 nm using an automated plate reader MRX<sup>TC</sup> revelation (Dyex Technologies, Inc., Chantilly, VA). The cell viability (%) was obtained by dividing the OD<sub>570</sub> value of the treated specimen by that of the untreated one.

**In vivo bone compatibility.**—The *in vivo* bone compatibility of the cements (EXPLC and Fuji II LC) was evaluated using five Spurge–Dawley rats weighing 350–400 g. The cement specimens were randomly implanted into the tibial medullary cavities with each tibia having one specimen. Three specimens for each material ( $n = 3$ ) were implanted for statistics. An empty cavity was used as control. The cement specimens with dimensions of 2 mm in diameter by 7 mm in length and surgical instruments were sterilized by autoclaving. The rats were induced by isoflurane inhalation followed by anesthetizing with a mixture of xylazine (10 mg kg<sup>-1</sup>) and ketamine (40 mg kg<sup>-1</sup>) through intra-peritoneal injection. Buprinorphine (0.1 mg kg<sup>-1</sup>) was given through intramuscular injection on the non-operated leg as an analgesic agent. Hairs on the right thigh were removed and the skins were prepared using a betadine disinfectant scrub alternating with 70% isopropyl alcohol rinses. A skin incision of 3 cm was made on the medial aspect of the right leg with surgical blades followed by a blunt dissection to reach the condylar surface of the knee joint. After locating the condylar surface, a dental bur was used to create a circular defect of 2 mm in diameter by about 10 mm in depth on the condylar surface into the medullary cavity under copious irrigation to avoid overheating. The specimens were then inserted into the medullary canal. After thorough irrigation of the operation field, the muscle layers and skin were closed with 3–0 Prolene with interrupted suture. The animals were allowed free movement after the surgery. After 7 days, animals were killed by inhalation of carbon dioxide followed by bilateral pneumothorax to ensure death. The tibia was processed for histomorphometry by washing, dehydrating in graded alcohols, and infiltrating and embedding in methyl methacrylate. Thin (7  $\mu\text{m}$ ) sections were taken through the cross section of each tibia using a rotating microtome (Reichert-Jung 2050, Reichert-Jung, Heidelberg, Germany). Alternating sections were stained with hematoxyline-and-eosin and McNeal's tetrachrome. Sections were viewed on a Nikon Optiphot fluorescence microscope (Nikon, Inc., Garden City, NJ).

Histomorphometry analysis was conducted using Bioquant imaging analysis software. The harvested implant specimen was removed during the preparation process and left a center hole in the bone tissues. The area of the center hole, which the implant used to occupy, was measured. A standard region of interest (ROI) of 3.58 mm<sup>2</sup> that covers approximately 200 μm<sup>2</sup> tissue surrounding the center hole was defined. The percentage of the area covered by mineralized bone in this ROI was measured from the tissue sectioned stained with McNeal stain. The percentage of the bone area was determined using the formula %bone area = total bone area/total tissue area.

**Statistical analysis.**—One-way analysis of variance (ANOVA) with the post hoc Tukey–Kramer multiple range test was used to determine significant differences of strengths, of *in vitro* cytotoxicity and of *in vivo* bone compatibility among the materials. A level of  $\alpha = 0.05$  was used for statistical significance.

## Results and discussion

### Characterization

The purified 6-arm BIBB initiator was a white crystal (melting point = 147–148 °C and yield = 63%). Its characteristic peaks from FT-IR (figure 2(a)) are listed as follows (cm<sup>-1</sup>). Carbonyl: 1740 (C=O stretching, strong) and 1271 (C–O–C stretching), C–Br: 1157 (C–Br bending), CH<sub>3</sub>: 1389, 1371, 1108 and 987 (CH<sub>3</sub> bending) and 2975–2900 (C–H stretching). For comparison, the characteristic peaks for BIBB are shown as follows. Carbonyl: 1808 and 1767 (C=O stretching, strong) and 944 (C=O bending); C–Br: 848, 626 and 599 (C–Br bending); CH<sub>3</sub>: 1459, 1371 and 1112 (CH<sub>3</sub> bending) and 2975–2950 (weak C–H stretching). It is clear that the significant shift of the carbonyl group from two peaks at 1808 and 1767 to one peak at 1738 and disappearances of 944 and 848 strongly confirmed the formation of the 6-arm BIBB, along with its clearly measured melting point (147–148 °C). The chemical shifts from <sup>1</sup>H NMR of the 6-arm BIBB initiator were found as follows (ppm): 4.29 (CH<sub>2</sub>), 3.59 and 1.94 (CH<sub>3</sub>). In contrast, BIBB only showed one chemical shift at 2.10.

The FT-IR spectra for t-BA, 6-arm poly(t-BA), 6-arm PAA and GM-tethered 6-arm PAA are shown in figure 2(b) and discussed below. t-BA shows multiple peaks in its spectrum. Among them, 1722 and 1636 are the two most characteristic peaks associated with carbonyl and carbon–carbon double bond, respectively. In contrast, disappearance of the peak at 1636 in the spectrum for the 6-arm poly(t-BA) confirmed the completion of polymerization. After hydrolysis of poly(t-BA), a broad and significant peak at 3600–2300 and a strong but wider peak at 1714.5 were observed as compared to poly(t-BA). The former is the typical peak for the hydroxyl group on carboxylic acid (OH stretching), whereas the latter is the characteristic peak for carbonyl stretching on PAA. In contrast, the GM-tethered PAA shows five typical peaks: 3600–2400 cm<sup>-1</sup> (OH stretching on COOH), 3434 (OH on tethered methacrylate), 1716.9 (C=O stretching on COO), 1636.1 (C=C bending) and 1508.4 (CH<sub>2</sub>C(OH)– asymmetrical deformation vibration from COOCH<sub>2</sub>C(OH)–). It is apparent that the peaks at 3434, 1636 and 1508 cm<sup>-1</sup> on the GM-tethered 6-arm PAA identified the difference between the 6-arm PAA and GM-tethered 6-arm PAA. The typical chemical shifts from <sup>1</sup>H NMR spectra for the 6-arm PAA and GM-tethered 6-arm PAA are listed as follows

(ppm). (1) 6-arm PAA: 12.25 (COOH), 3.4 (CH<sub>2</sub>), 2.25 (CH), 1.8 and 1.55 (CH<sub>2</sub>), and 1.1 (CH<sub>3</sub>). (2) The GM-tethered 6-arm PAA: 12.30 (COOH) and 5.70 and 6.10 (C=CH<sub>2</sub>). The characteristic chemical shifts at 5.70 and 6.10 identified the difference between the above two polymers.

Table 1 shows the conversions and molecular weights (MWs) of the 6-arm PAA and linear PAA. The conversions of the 6-arm PAA and linear PAA were determined using FT-IR spectra and they were 98.7% and 99.9%, respectively. The MW of the synthesized 6-arm PAA was 15 361 Daltons (determined by <sup>1</sup>H NMR). Briefly, the 6-arm PAA (0.5%) was dissolved in d-DMSO for <sup>1</sup>H NMR. The peaks from 4.10 to 4.39 ppm were assigned to the hydrogen atoms of the –CH<sub>2</sub>– groups in a 6-arm BIBB unit, with the integration set as 12 H. The peaks from 0.86 to 3.96 ppm were assigned to the hydrogen atoms on the PAA carbon skeleton, with an integration of 592.3 H. Since a full conversion would yield 600 H on the carbon skeleton, the conversion was calculated to be 98.7% (592.3/600 × 100%). The formula for the calculation of MW = MW<sub>initiator</sub> + MW<sub>AA</sub>/concentration<sub>initiator</sub> × conversion. The MW (15 361) determined from <sup>1</sup>H NMR was very close to the calculated MW (15 560). The MW of the linear PAA via conventional free-radical polymerization was 9704 (determined by VPO).

## Synthesis

**Synthesis of the 6-arm PAA.**—It is known that almost all the poly(alkenoic acid)s being used in current dental GICs are linear polymers and synthesized via conventional free-radical polymerization. No reports have been found so far on the study of different architectures of polyacids for GIC applications. One of the main reasons may be attributed to the fact that it is impossible to synthesize polymers with different architectures by using conventional free-radical polymerization techniques. ATRP, a recently developed technology for controlled radical polymerization, is capable of making various architectures such as star polymers and block copolymers [21]. By using such a technique, we were able to synthesize novel star-shaped (or spherical) PAA in this study. Figure 3 shows a semi-logarithmic plot of ATRP of t-BA in dioxane (straight line) and a kinetic plot of monomer-to-polymer conversion versus time (curve). The polymerization was initiated by the 6-arm BIBB, catalyzed by the CuBr-PMDETA complex and run at 120 °C. The plot of ln([M]<sub>0</sub>/[M]) versus time (straight line), where [M]<sub>0</sub> = the initial concentration of the monomer and [M] = the monomer concentration at any time, is almost linear, suggesting that the polymerization propagation was constant throughout the reaction or, in other words, a constant concentration of growing radicals reflects a first-order kinetics. From the kinetic plot of monomer-to-polymer conversion versus time (curve), it is apparent that the monomer conversion increased with time. The reaction in dioxane took 3 h to reach a 90.9% conversion and 5 h to reach a 97.6% conversion. In order to make sure that the t-BA was polymerized only by ATRP and not by heat-initiated conventional free-radical polymerization, a parallel experiment without any initiator involved was conducted under the same condition. It was found that no polymer was generated within 8 h, which indicates that poly(t-BA) was polymerized by the ATRP reaction. The 6-arm PAA was prepared by hydrolysis of poly(t-BA) in a mixed solvent of dioxane and aqueous HCl (37%) for 10 h

under a refluxed condition [29], followed by dialysis against water until the pH reached neutral.

**Synthesis of the GM-tethered 6-arm PAA.**—The reaction between GM and carboxylic acid on PAA took about 14 h to complete. Disappearance of the epoxy group on GM at  $761\text{ cm}^{-1}$  from FT-IR confirmed the completion of the tethering reaction. The completion of the tethering of GM was also confirmed by the fact that the yield was greater than 95%.

## Evaluation

**Significance of synthesis of the 6-arm PAA and tethering of GM onto the 6-arm PAA.**—The main difference between LCGIC and CGIC is their liquid composition [4]. The liquid in LCGIC is composed of HEMA, photo-initiators, water and a poly(alkenoic acid) having pendent *in situ* polymerizable methacrylate on its backbone [12, 14] or a mixture of poly(alkenoic acid) and methacrylate-containing monomer/oligomer [13]. The liquid in CGIC consists of only hydrophilic poly(alkenoic acid) and water [1, 2]. Due to the introduction of hydrophobic methacrylate functionality, amphiphilic monomers such as HEMA have to be incorporated into the LCGIC liquid formulation to enhance the solubility of the hydrophobic methacrylate-containing poly(alkenoic acid) in water, although HEMA has demonstrated cytotoxicity to cells [22, 24–26]. Without these amphiphilic small molecules, however, it seems impossible to formulate LCGICs by using current technologies [1, 4]. Our previous research has shown that tethering GM onto the poly(alkenoic acid) backbone can increase water solubility of the polyacid due to an introduction of hydroxyl groups [35] (see figure 1(c)), as compared to 2-isocyanatoethyl methacrylate (IEM)-tethered poly(alkenoic acid) [12, 14, 17]. If we take a close look at the chemical structure of the GM-tethered 6-arm PAA (figure 1(c)), it is apparent that when the epoxy group on GM reacts with the carboxyl group on PAA, a pendant hydroxyl-containing methacrylate group, i.e.  $\text{CH}_2=\text{C}(\text{CH}_3)\text{COO}-\text{CH}_2\text{CH}(\text{OH})-\text{CH}_2\text{OOC}-$ , forms. In other words, when the GM molecule is grafted onto the PAA backbone, it produces one extra hydroxyl group. In contrast, when the isocyanate group on IEM reacts with the carboxyl group on PAA, the amide linkage, i.e.  $\text{CH}_2=\text{C}(\text{CH}_3)\text{COO}-\text{CH}_2\text{CH}_2\text{HNOC}-$ , forms with the evolution of carbon dioxide. Unlike IEM tethering, these hydroxyl groups should make the GM-tethered PAA less hydrophobic. However, we also noted that these hydroxyl groups might reduce the mechanical strength and increase the viscosity. This is because on one hand these hydroxyl groups can absorb water and serve as a hydrogel, which might lead to a strength reduction, but on the other hand they can make a contribution to hydrogen bond formation, which might result in an increased viscosity. To overcome these shortcomings, we proposed the following two strategies: (1) using the star-shaped 6-arm PAA for a reduced viscosity, which has been proven valid [20], and (2) increasing the polymer content in the liquid formulation to offset the reduced mechanical strengths that might be caused by these hydroxyl groups, because the more the polymer in the formulation, the higher the mechanical strengths [15]. It is apparent from tables 1 and 2 that the 6-arm PAA showed a significantly reduced solution viscosity (950.4–3323 cP, see table 2) even at a much higher MW (15 272 Daltons) as compared to its linear counterpart (6830 cP, 9704 Daltons, see tables 1 and 2).

**Effects of the polymer/water (P/W) ratio and grafting ratio on compressive**

**properties.**—To study the effects of the P/W ratio (by weight) and grafting ratio (by mole, grafting ratio = moles of GM added divided by moles of carboxylic acid groups on the polymer) on strengths, we formulated six liquid solutions (A to F) based on the 6-arm PAA tethered with GM and one liquid solution (G) based on the linear PAA tethered with GM. Three P/W ratios including 50/50, 60/40 and 75/25 and two grafting ratios including 35% and 50% were studied. Table 2 shows the yield compressive strength (YS), modulus, ultimate compressive strength (UCS) and viscosity values of the cements prepared from the above formulations. The cements A, B and C represent the 35% GM-tethered 6-arm PAAs with the P/W ratios at 50/50, 60/40 and 75/25 respectively. It is obvious that an increasing P/W ratio significantly increased YS, modulus and UCS, indicating that a higher polymer concentration can enhance the mechanical strengths of the relative hydrophilic GM-tethered PAA cement. Meanwhile, the viscosity of the polymer solution was also increased due to increased polymer contents. The cement A showed the lowest YS (29.6 MPa), modulus (2.55 GPa) and UCS (63.9 MPa), which implies that at 50/50, the hydrophilic characteristic of the GM-tethered PAA prevails and the cement behaves like a hydrogel. However, an increasing polymer content in water overcomes the disadvantage exhibited by the hydroxyl groups from the GM-tethered PAA and makes the cement stronger. Considering the effect of the grafting ratio on the strength, increasing the grafting ratio significantly increased YS, modulus and UCS. The cement F with the P/W ratio = 75/25 and grafting ratio = 50% was the highest in YS, modulus and UCS. The reason can be attributed to the fact that the higher the grafting ratio, the more the carbon-carbon double bonds in the GM-tethered polymer, thus leading to a higher mechanical strength. This result is very encouraging because it has demonstrated the feasibility of eliminating low MW comonomers in LCGIC formulations, which may greatly improve the biocompatibility of current commercially available light-cured GICs. We also noted that the viscosity values were increased when the P/W ratio increased. Furthermore, the polymer solutions with 35% GM showed a much higher viscosity as compared to those with 50% GM, which can be attributed to a relatively strong hydrogen bond formation in the polymer solutions with 35% GM because less GM tethering means more free acids attached to the polymer backbone. In contrast, the linear PAA (G) that was synthesized via conventional free-radical polymerization showed much lower strengths (YS = 105.4 MPa, modulus = 5.43 GPa and UCS = 124.5) but much higher viscosity (6830 cP) than those for the corresponding 6-arm PAA cement F (186.3 MPa, 7.32 GPa, 277.9 MPa and 950.4 cP), even though the former had much lower MW (9704 Daltons in table 1) than the latter (15 272 Daltons). As we know, it is hard to increase strengths of the linear PAA only by increasing the MW because increasing MW increases hydrogen bond formations resulting from the ordered linear PAA structure [2, 16, 18]. The present result indicates that the 6-arm PAA can overcome the shortcoming generated by the ordered linear PAA.

**Effect of the glass powder/polymer liquid ratio on compressive properties.**—

The glass powder/polymer liquid (P/L) ratio is one of the most important parameters in formulating GICs [2, 4]. Usually a higher P/L ratio results in higher mechanical strengths, especially CS [36, 37], but it also shortens the working time [2]. Since the working time is not a problem for a light-curable GIC system, a higher P/L ratio is used in some LCGICs,

such as Fuji II LC (P/L = 3.2). In the present study, we investigated the effect of three P/L ratios (2.2, 2.7 and 3.0) on CS. As shown in figure 4, the strength was in a decreasing order: (YS)  $2.7 (186.3 \pm 2.9) > 3.0 (173.8 \pm 6.8) > 2.2 (162.9 \pm 8.5)$ , where 2.2, 2.7 and 3.0 were not significantly different from each other; (UCS)  $2.7 (277.9 \pm 11.7) > 3.0 (274.9 \pm 9.8) > 2.2 (244.1 \pm 12)$ , where 2.2, 2.7 and 3.0 were not significantly different from each other; (modulus)  $3.0 (8.09 \pm 0.13) > 2.7 (7.32 \pm 0.23) > 2.2 (6.72 \pm 0.06)$ . It seems that a P/L ratio had no influence on YS and UCS except for modulus. An increase in modulus can be attributed to a higher filler content. It is worth pointing out that we experienced somewhat a mixing difficulty with the P/L ratio = 3.0 when preparing the cement specimens, which might cause a lower CS.

**Aging.**—GICs usually increase their strengths with time in the presence of water due to constant salt-bridge formations [3, 38]. In the present study, we evaluated EXPLC and Fuji II LC by testing the CS of specimens in the course of aging after specimens were conditioned in distilled water at 37 °C. The results are shown in figure 5 and table 3. EXPLC showed a significant increase in CS or UCS (MPa) from 210.9 at 1 h to 277.9 at 1 day (a 32% increase) and from 277.9 at 1 day to 323.3 at 1 week (a 16% increase). Fuji II LC showed only a 15% increase from  $181.5 \pm 12$  at 1 h to 212.7 at 1 day, followed by a 3% increase from 212.7 at 1 day to 219.1 at 1 week. The above results indicate that the salt-bridge formation in Fuji II LC cement was mainly complete within a 24 h period. However, the continuous increase in CS by EXPLC from 1 day to 1 week may be partially attributed to the nature of the 6-arm PAA's spherical structure. We infer that in the 6-arm PAA-composed cement, the salt-bridge formation may start gradually from the outside toward the inside, which requires more time to complete. That is why a continuous increase in CS from 1 day to 1 week was observed. Similar behaviors can also be observed from the results for YS and modulus, as shown in table 3. The significantly higher initial UCS (210.9 MPa at 1 h) combined with a continuous increase exhibited by EXPLC will make this novel cement system attractive to restorative dentistry.

**Property comparison between the experimental and commercial cements.**—To identify how good the newly developed cement system is, we compared the CS, DTS, FS, FT and shrinkage of EXPLC with those of Fuji II LC. The strengths of these cements were determined after they were conditioned in distilled water at 37 °C for 1 week. As shown in table 4, EXPLC showed significantly higher CS, DTS, FS and FT as compared to Fuji II LC. EXPLC were 48% in CS, 77% in DTS, 95% in FS and 59% in FT higher than Fuji II LC. Regarding shrinkage, EXPLC showed a much lower value (0.9) as compared to Fuji II LC (4.7). Higher mechanical strengths exhibited by EXPLC can be attributed to the nature of this unique high polymer content and comonomer-free system. The high polymer content provides not only a large quantity of carboxyl groups for salt-bridge formations but also a substantial amount of a carbon-carbon double bond for covalent crosslinks. In contrast, the Fuji II LC system contains low MW HEMA and/or other methacrylate comonomers [13]; these low MW molecules cause lower mechanical strengths and higher shrinkage. The significantly lower shrinkage exhibited by EXPLC may be attributed to the pendent hydroxyl groups. These hydrophilic hydroxyl groups may offset the shrinkage produced by both polymerization of carbon-carbon double bonds and salt-bridge formation.

**In vitro and in vivo biocompatibility.**—It is known that resin-modified or light-cured glass-ionomer cements (RMGICs or LCGICs) are less biocompatible than CGICs [22, 23]. Leachables from LCGICs have shown adverse effects on cell viability and thus caused cytotoxicity [22, 24, 39], although glass ionomers are generally considered as inert materials as compared to dental composite resins. The MTT assay has been the most popular and commonly used tool for evaluation of cytotoxicity of the biomaterials [8]. As we know, CGICs are composed of poly(carboxylic acid)s, water and calcium fluoroaluminosilicate glass powders [2], whereas LCGICs contain polymerizable polyacid or a mixture of polyacid and dimethacrylates, HEMA, water and calcium fluoroaluminosilicate glass powder [4, 12, 13]. It has been found that CGICs often show very little *in vitro* cytotoxicity, but LCGICs exhibit significantly higher cytotoxicity as compared to CGICs [22, 23, 39]. The reason is mainly attributed to HEMA and the incorporated photo-initiators and activators [22, 39]. Theoretically speaking, our experimental cement should not show any significant cytotoxicity and its biocompatibility should be similar to that of those CGICs since the experimental cement does not contain any comonomers in its formulation. Figure 6 shows the cell viability after the cells were cultured with the eluates of the two materials tested and blank, i.e. negative control (NC). NC showed the highest cell viability, but Fuji II LC showed the lowest viability after cell exposure to 7 day eluates. The viability (%) was in the decreasing order: NC ( $98.1 \pm 6.7$ ) > EXPLC ( $93.4 \pm 0.8$ ) > Fuji II LC ( $31.7 \pm 7.8$ ), where NC and EXPLC were not significantly different from each other. EXPLC showed significantly high cell viability as compared to Fuji II LC GIC. This can be attributed to the fact that EXPLC contains no comonomers before polymerization, and thus no leachables (unreacted monomers) should be expected. Fuji II LC was found to contain a substantial amount of HEMA in its liquid formulation by gas chromatography [39].

Regarding the *in vivo* bone compatibility, we found that the percentage (%) trabecular bone area ( $38.0 \pm 6.0$ ) surrounding the experimental cement (EXPLC) was much higher than that ( $12.0 \pm 7.0$ ) surrounding Fuji II LC after 7 day implantation (see figure 7). No inflammation reaction was found in tissue space next to either EXPLC or Fuji II LC cement implant. It seems that this novel experimental cement is more bone compatible than Fuji II LC after implantation in a tibia medullary cavity.

According to the above *in vitro* and *in vivo* results, it can be concluded that the experimental cement is not only stronger but also more biocompatible than Fuji II LC.

## Conclusions

We have developed a novel high-strength light-cured GIC based on the 6-arm PAA tethered with glycidyl methacrylate. The 6-arm PAA polymer was synthesized using ATRP. The synthesized 6-arm polymer showed a lower viscosity as compared to its linear counterpart that was synthesized via conventional free-radical polymerization, which is probably attributed to the spherical nature of the former. The effect of the polymer/water (P/W) ratio was significant, i.e. an increasing P/W ratio significantly increased YS, modulus and UCS. The effect of the P/L ratio was not significant, except for modulus. In the course of aging, the experimental cement showed a significant and continuous increase in YS, modulus and UCS within 1 week but Fuji II LC only showed a significant increase in

strength within 24 h. Furthermore, the experimental cement showed significantly higher mechanical strengths including YS, modulus, UCS, DTS, FS and FT and lower shrinkage, as compared to Fuji II LC. The experimental cement was also very biocompatible *in vivo* to bone and showed little *in vitro* cytotoxicity, as compared to Fuji II LC. It appears that this novel comonomer-free LCGIC cement will be a better dental restorative because it demonstrated significantly improved mechanical strengths and better *in vitro* and *in vivo* biocompatibilities as compared to the current commercial LCGIC system. Future studies will focus on optimization of the system, evaluation of other properties such as bonding to tooth, water sorption and fluoride release.

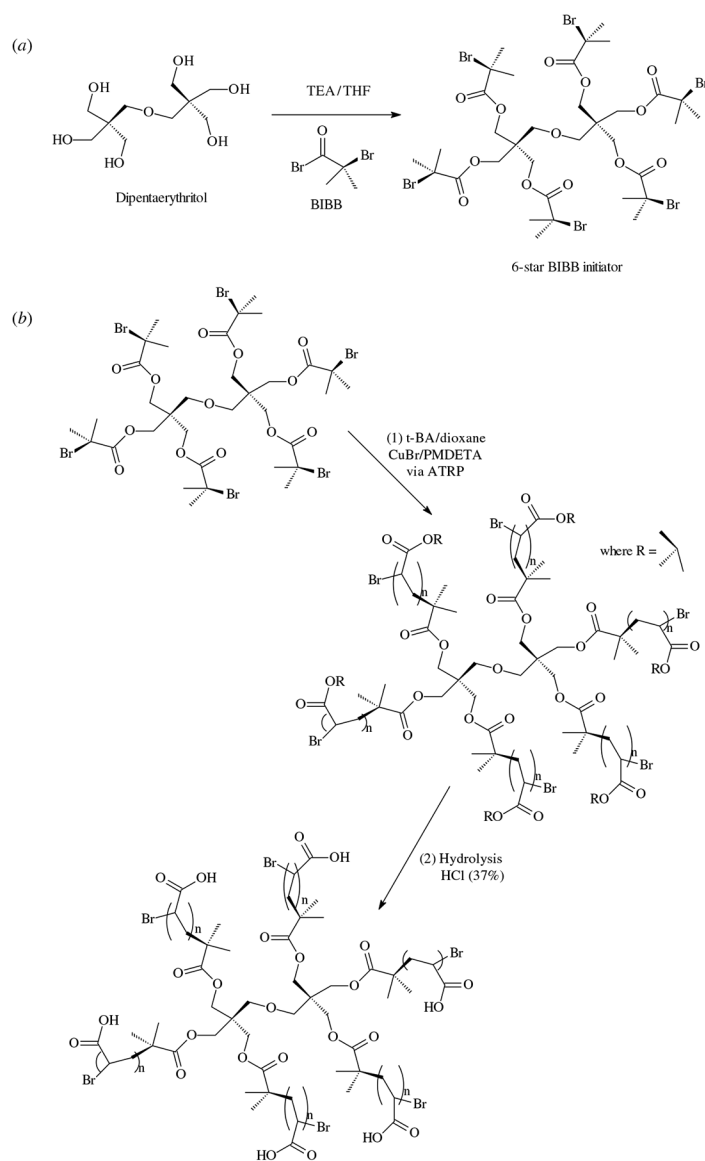
## Acknowledgments

This work was sponsored by NIH grant DE018333. Dr Yang was partially supported by NRSA (NIH T32HL07910). The authors would also like to give special thanks to GC America Inc. for its generous supply of Fuji II LC glass powders.

## References

- [1]. Smith DC 1998 *Biomaterials* 19 467–78
- [2]. Wilson AD and McLean JW 1988 *Glass-Ionomer Cements* (Chicago: Quintessence)
- [3]. Davidson CL and Mjör IA 1999 *Advances in Glass-Ionomer Cements* (Chicago: Quintessence)
- [4]. Wilson AD 1990 *Int. J. Prosthodont* 3 425–9 [PubMed: 2088379]
- [5]. Hotz P, McLean JW, Sced I and Wilson AD 1977 *Br. Dent. J* 142 41–7 [PubMed: 318839]
- [6]. Lacefield WR, Reindl MC and Retief DH 1985 *J. Prosthet. Dent* 53 194–8 [PubMed: 3884786]
- [7]. Forsten L 1977 *Scand. J. Dent. Res* 85 503–4 [PubMed: 271348]
- [8]. Craig RG 1997 *Restorative Dental Materials* 10th edn (St Louis: Mosby-Year Book)
- [9]. Nicholson JW, Braybrook JH and Wasson EA 1991 *J. Biomater. Sci. Polym. Edn* 2 277–85
- [10]. Hume WR and Mount GJ 1988 *J. Dent. Res* 67 915–8 [PubMed: 3170904]
- [11]. Guggenberger R, May R and Stefan KP 1998 *Biomaterials* 19 479–83 [PubMed: 9645553]
- [12]. Mitra SB 1991 *J. Dent. Res* 70 72–4 [PubMed: 1991864]
- [13]. Momoi Y, Hirotsaki K, Kohno A and McCabe JF 1995 *Dent. Mater. J* 14 109–19 [PubMed: 8940550]
- [14]. Xie D, Culbertson BM and Johnston WM 1998 *J. M. S. Pure Appl. Chem. A* 35 1631–50
- [15]. Xie D, Wu W, Puckett A, Farmer B and Mays J 2004 *Eur. Polym. J* 40 343–51
- [16]. Kao EC, Culbertson BM and Xie D 1996 *Dent. Mater* 12 44–51 [PubMed: 8598250]
- [17]. Xie D, Chung I-D, Wu W, Lemons J, Puckett A and Mays J 2004 *Biomaterials* 25 1825–30 [PubMed: 14738846]
- [18]. Xie D, Culbertson BM and Johnston WM 1998 *J. M. S. Pure Appl. Chem. A* 35 1615–29
- [19]. Bahadur P and Sastry NV 2002 *Principles of Polymer Science* (Boca Raton, FL: CRC Press)
- [20]. Huang CF, Lee HF, Kuo SW, Xu H and Chang FC 2004 *Polymer* 45 2261–9
- [21]. Matyjaszewski K and Xia J 2001 *Chem. Rev* 101 2921–90 [PubMed: 11749397]
- [22]. de Souza Costa CA, Hebling J, Garcia-Godoy F and Hanks CT 2003 *Biomaterials* 24 3853–8 [PubMed: 12818558]
- [23]. Leyhausen G, Abtahi M, Karbakhsch M, Sapotnick A and Geustsen W 1998 *Biomaterials* 19 559–64 [PubMed: 9645563]
- [24]. Stanislawski L, Daniau X, Lauti A and Goldberg M 1999 *J. Biomed. Mater. Res* 48 277–88 [PubMed: 10398031]
- [25]. Oliva A, Della Ragione F, Salerno A, Riccio V, Tartaro G, Cozzolino A, D'Amato S, Pontoni G and Zappia V 1996 *Biomaterials* 17 1351–6 [PubMed: 8805985]

- [26]. Ratner BD, Hoffman AS, Schoen FJ and Lemons JE 1996 *Biomaterials Science, An Introduction to Materials in Medicine* (San Diego, CA: Academic)
- [27]. Wang X, Zhang H, Zhong G and Wang X 2004 *Polymer* 45 3637–42
- [28]. Ibrahim K, Lofgren B and Seppala J 2003 *Eur. Polym. J* 39 2005–10
- [29]. Davis KA, Charleux B and Matyjaszewski K 2000 *J. Polym. Sci. A* 38 2274–83
- [30]. Xie D, Faddah M and Park JG 2005 *Dent. Mater* 21 739–48 [PubMed: 15882900]
- [31]. Johnson WW, Dhuru VB and Brantley WA 1993 *Dent. Mater* 9 95–8 [PubMed: 8595849]
- [32]. Wang G, Culbertson BM, Xie D and Seghi RR 1999 *J. M. S. Pure Appl. Chem. A* 36 237–52
- [33]. Wataha JC, Rueggeberg FA, Lapp CA, Lewis JB, Lockwood PE, Ergle JW and Mettenburg DJ 1999 *Clin. Oral Invest* 3 144–9
- [34]. Yang Y, Chen Q and Zhang JT 2002 *J. Biol. Chem* 277 44268–77 [PubMed: 12235150]
- [35]. Xie D, Park JG and Faddah M 2006 *J. Biomater. Sci. Polym. Edn* 17 303–22
- [36]. Xie D, Brantley WA, Culbertson BM and Wang G 2000 *Dent. Mater* 16 129–38 [PubMed: 11203534]
- [37]. Xie D, Culbertson BM and Wang G 1998 *J. M. S. Pure Appl. Chem. A* 35 547–61
- [38]. Cattani-Lorente MA, Godin C and Meyer JM 1994 *Dent. Mater* 10 37–44 [PubMed: 7995474]
- [39]. Geurtsen W, Spahl W and Leyhausen G 1998 *J. Dent. Res* 77 2012–9 [PubMed: 9839790]



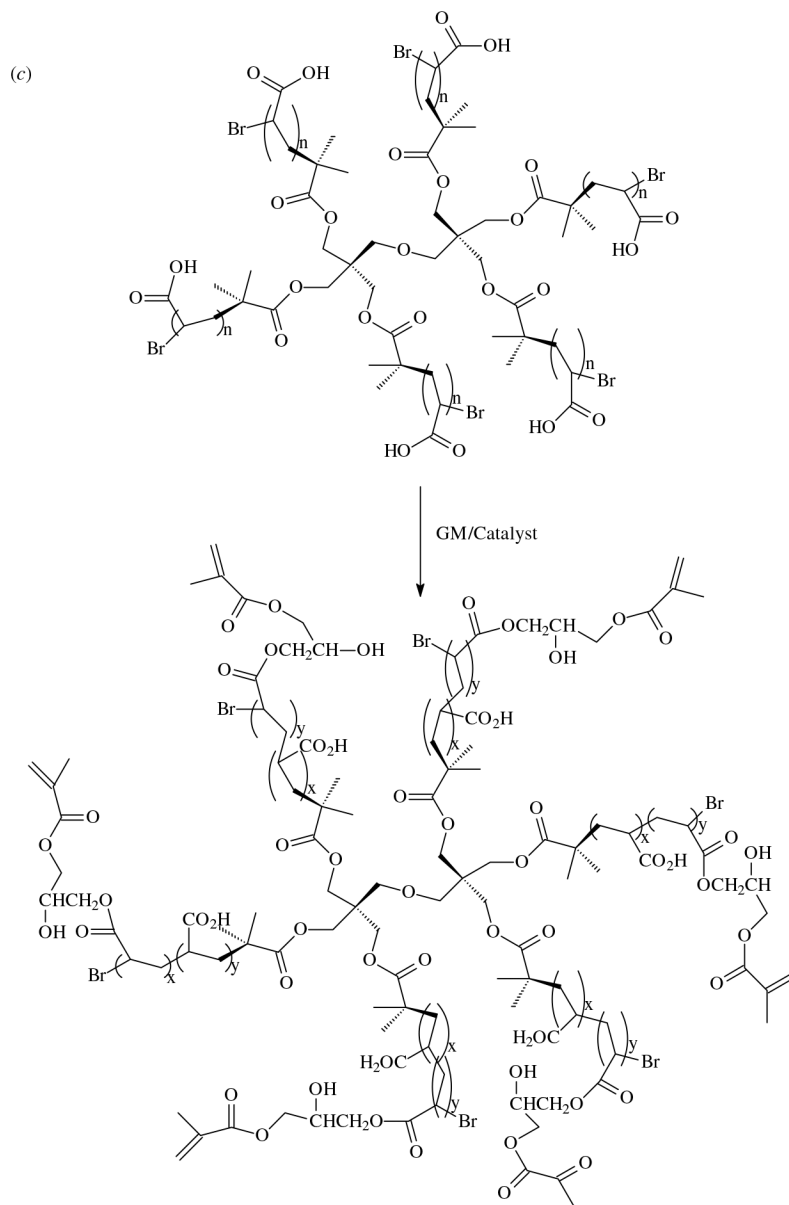


**Figure 1.** Schematic diagram for synthesis: (a) synthesis of the 6-arm initiator, (b) synthesis of the 6-arm poly(*t*-BA) via ATRP and formation of the 6-arm PAA and (c) GM tethering.

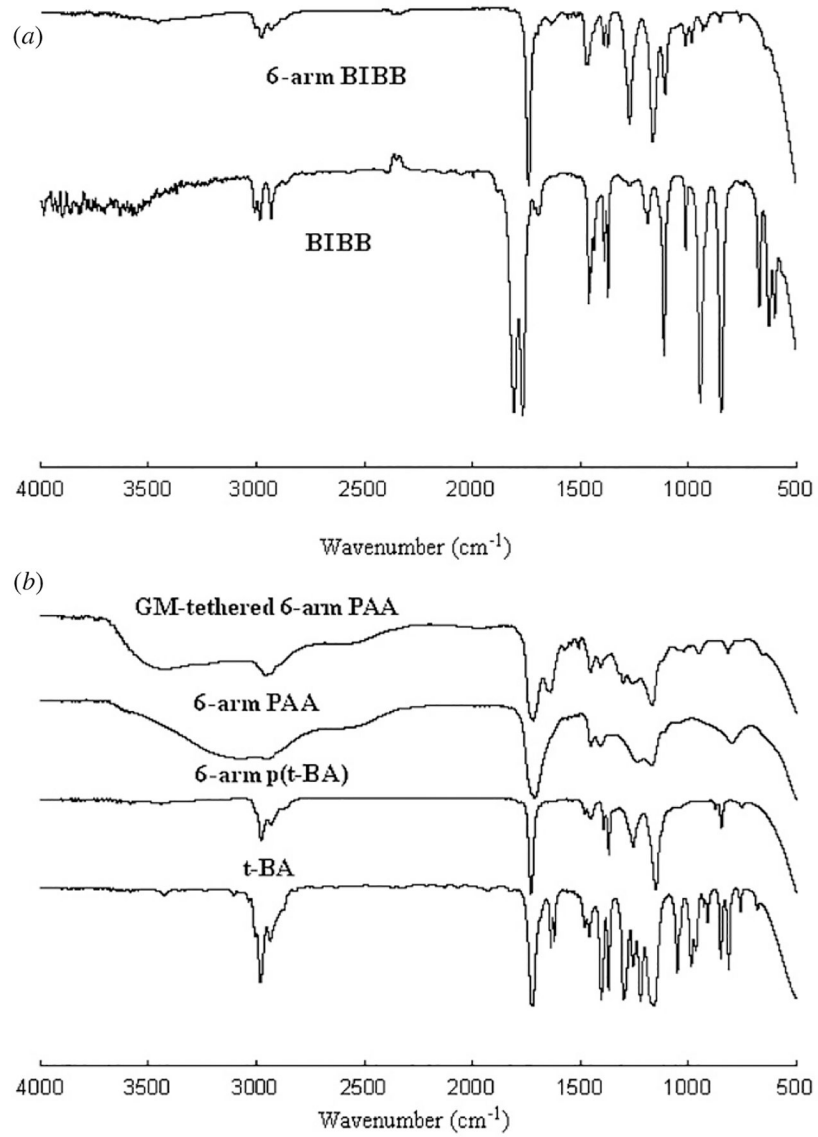


**Figure 2.** FT-IR spectra for the initiator and polymers: (a) BIBB and 6-arm BIBB initiator, (b) t-BA, 6-arm p(t-BA), 6-arm PAA and GM-tethered 6-arm PAA.

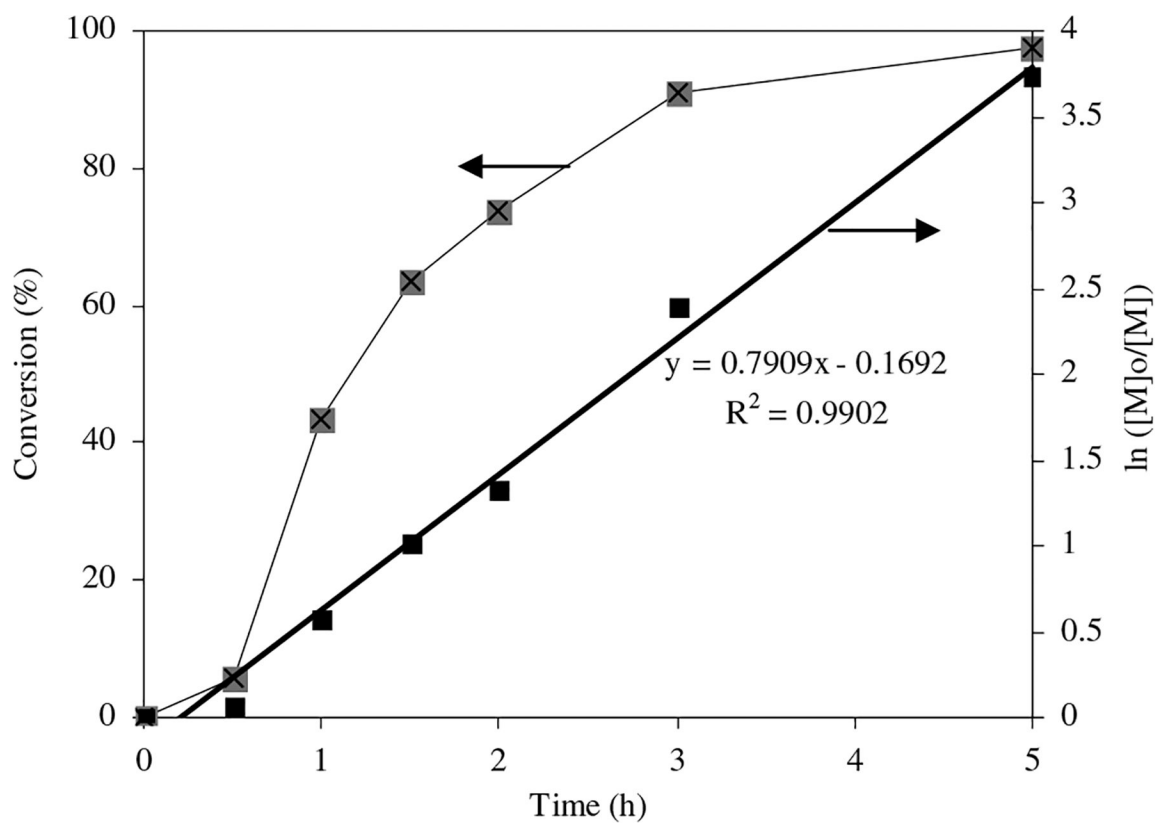


**Figure 3.**

Conversion and kinetic plot of the 6-arm poly(t-BA) derived from the FT-IR absorbance spectra. Top: conversion versus time curve, bottom: first-order kinetic plot of  $\ln([M]_0/[M])$  versus time. The 6-arm poly(t-BA) was prepared in dioxane via ATRP in the presence of the 6-arm BIBB, CuBr and PMDETA.

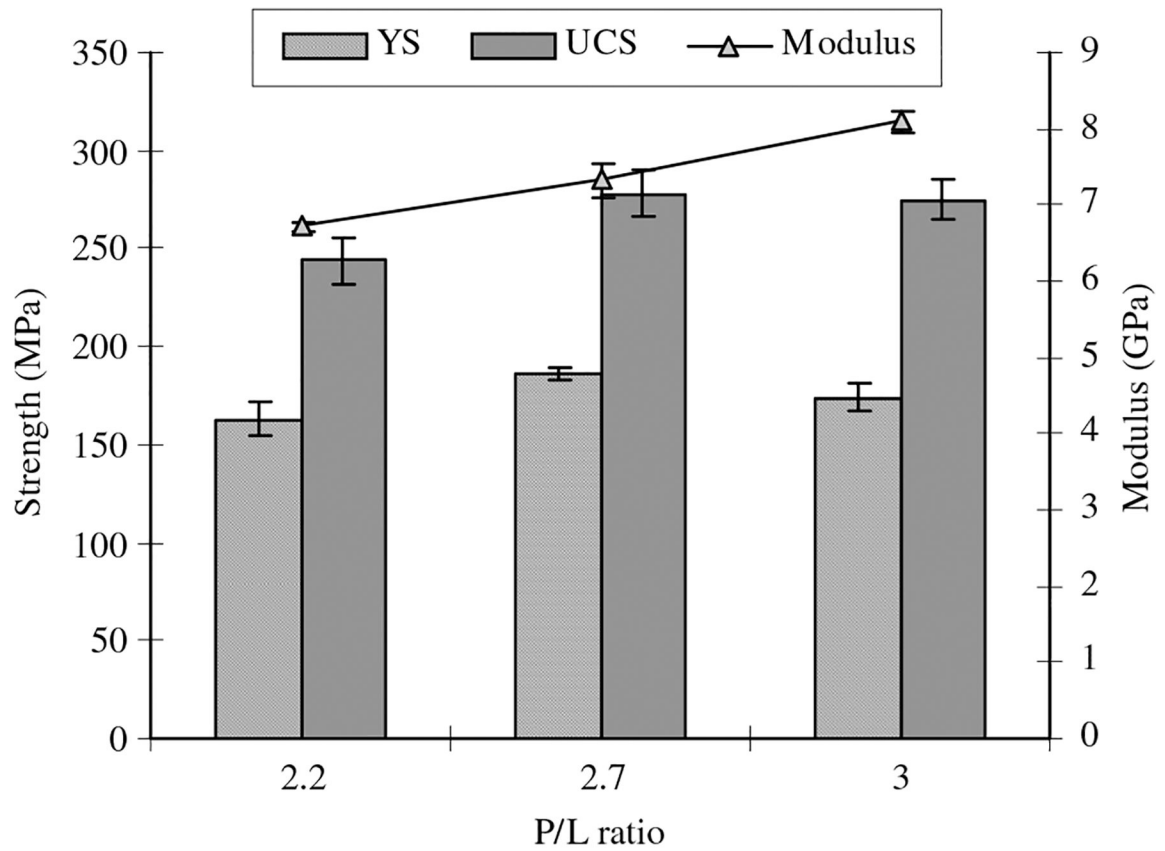


**Figure 4.** Effect of the glass powder/polymer liquid (P/L) ratio on CS: MW of the 6-arm PAA = 15 272 Daltons; filler = Fuji II LC; grafting ratio = 50% (by mole); P/W ratio = 75:25 (by weight). Specimens were conditioned in distilled water at 37 °C for 24 h.

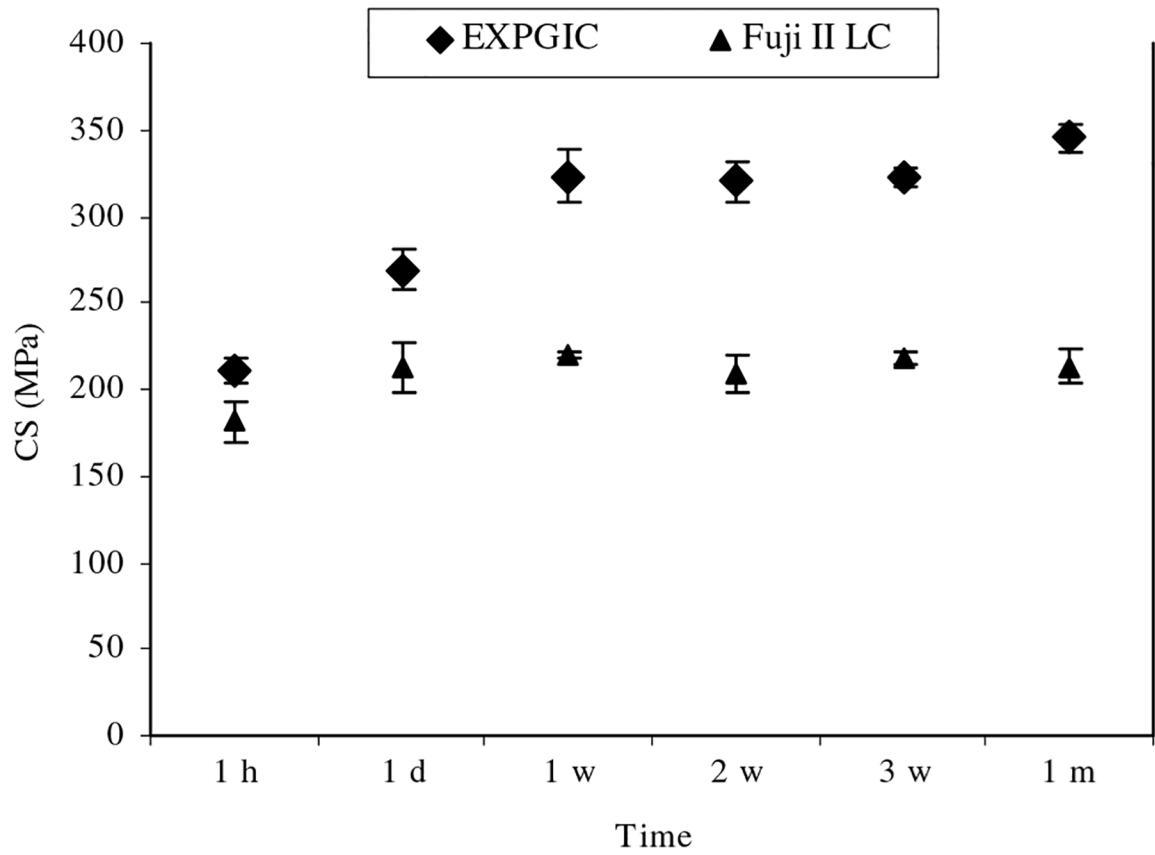


**Figure 5.** Effect of aging on CS: MW of the 6-arm PAA = 15 272 Daltons; filler = Fuji II LC; grafting ratio = 50%; P/L ratio = 2.7. P/W ratio = 75:25. Specimens were conditioned in distilled water at 37 °C prior to testing.

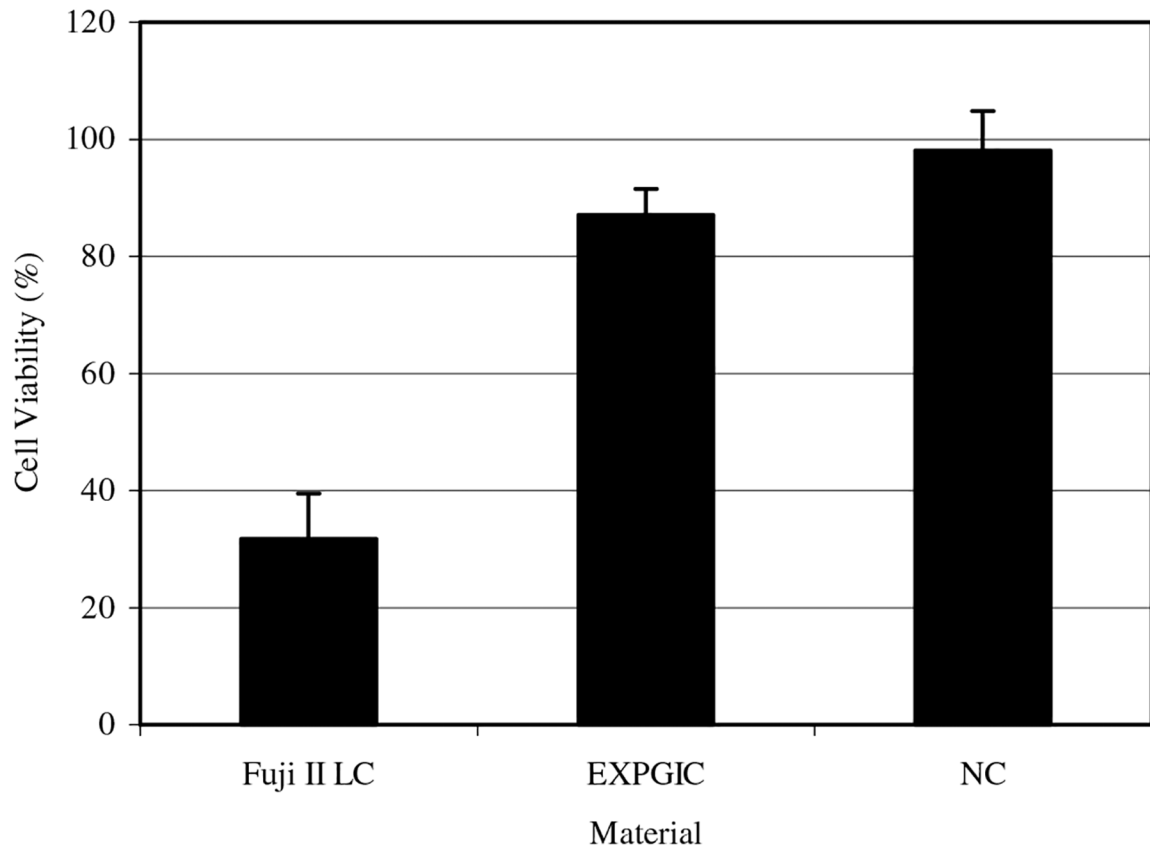


**Figure 6.**

Cell viability comparison after culturing with the eluates from different cements for 3 days. Eluates were obtained from the 3-day and 7-day incubation at a concentration of 80%. For EXPLC, the MW of the 6-arm PAA = 15 272 Daltons; filler = Fuji II LC; grafting ratio = 50%; P/L ratio = 2.7. P/W ratio = 75:25.

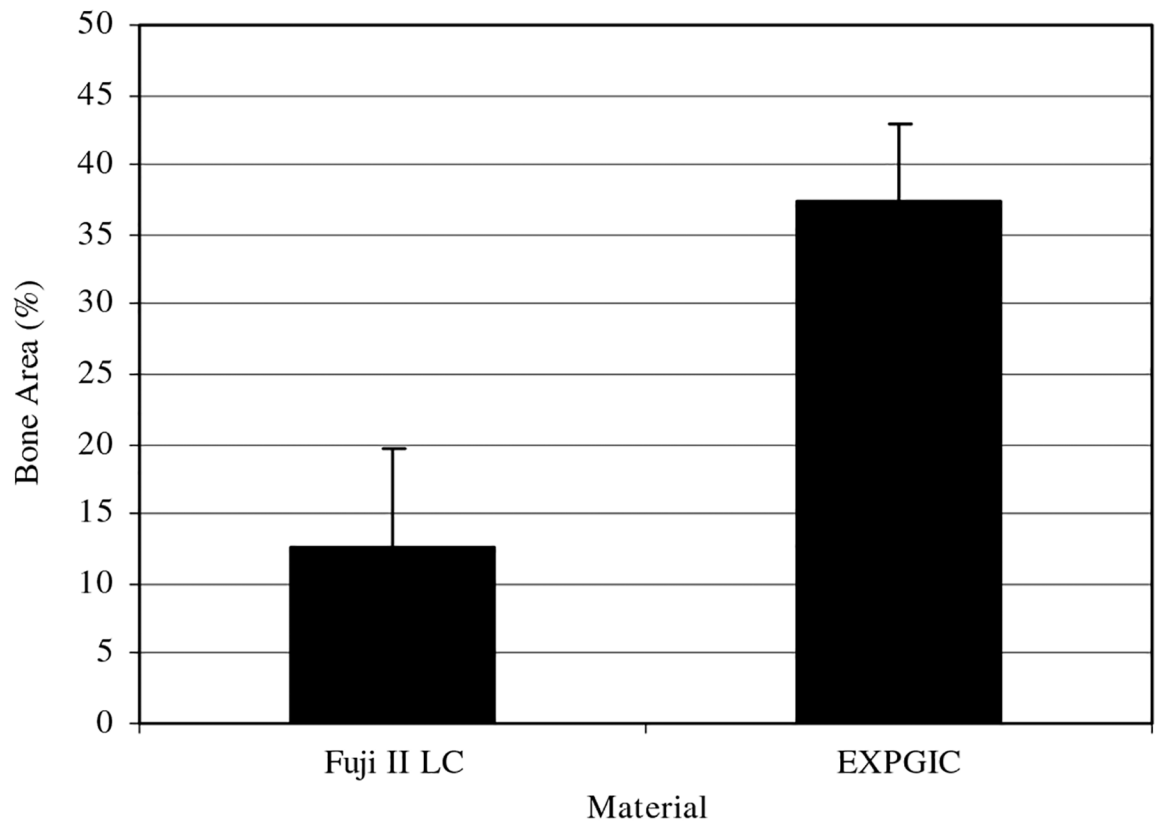


**Figure 7.**

*In vivo* bone compatibility comparison after the cements were implanted in Spurge–Dawley rats for 7 days. The percentage bone area in a defined 3.58 mm<sup>2</sup> region of interest surrounding the cement implants was calculated. For EXPLC, the MW of the 6-arm PAA = 15 272 Daltons; filler = Fuji II LC; grafting ratio = 50%; P/L ratio = 2.7. P/W ratio = 75:25.

**Table 1.**

Conversion, MW and viscosity of synthesized PAAs.

Polymer	Conversion <sup>a</sup> (%)	MW
6-arm	98.7	15 361 <sup>b</sup>
Linear	99.9	9 704 <sup>c</sup>

<sup>a</sup>Conversions were measured from FT-IR spectra.<sup>b</sup>MW of 6-arm PAA was determined by <sup>1</sup>H NMR.<sup>c</sup>MW of linear PAA was estimated in DMF via a vapor pressure osmometer.

Author Manuscript

Author Manuscript

Author Manuscript

Author Manuscript

**Table 2.**Effects of the polymer/water ratio and GM grafting ratio on compressive properties<sup>a</sup>.

Code	P/W ratio	Grafting ratio (%)	YS <sup>b</sup> (MPa)	Modulus (GPa)	UCS <sup>c</sup> (MPa)	Viscosity <sup>d</sup> (cP)
A	50/50	35	29.6 (2.1)	2.55 (0.06)	63.9 (2.9)	68.0
B	60/40	35	48.2 (1.4) <sup>a,e</sup>	3.35 (0.21)	104.4 (0.5) <sup>d</sup>	240
C	75/25	35	103.6 (1.6) <sup>b</sup>	5.51 (0.16) <sup>c</sup>	167.2 (4.2)	3323
D	50/50	50	48.8 (3.4) <sup>a</sup>	2.89 (0.44)	97.3 (2.7) <sup>d</sup>	18.5
E	60/40	50	77.5 (0.3)	4.53 (0.02)	129.2 (3.1) <sup>e</sup>	58.9
F	75/25	50	186.3 (2.9)	7.32 (0.23)	277.9 (12)	950.4
G	75/25	50	105.4 (7.7) <sup>b</sup>	5.43 (0.34) <sup>c</sup>	126.5 (7.7) <sup>e</sup>	6830

<sup>a</sup>MW of the 6-arm PAAAs (A–F) = 15 272 Daltons, G = linear PAA, which was synthesized via conventional free-radical polymerization and tethered with GM, MW of G = 9704 Daltons, filler = Fuji II LC, grafting ratio = 50% (by mole), P/W ratio = 75:25 (by weight).

<sup>b</sup>YS = CS at yield.

<sup>c</sup>UCS = Ultimate CS.

<sup>d</sup>Viscosity of the GM-tethered polymer/water solution was determined at 23 °C.

<sup>e</sup>Entries are mean values with standard deviations in parentheses and the mean values with the same superscript letter were not significantly different ( $p > 0.05$ ). All the specimens were conditioned in distilled water at 37 °C for 24 h.

**Table 3.**

Yield CS, modulus, ultimate CS in the course of aging.

Material <sup>a</sup>	1 h	1 d	1 w	2 w	3 w	1 m
	Y <sub>S</sub> <sup>b</sup> (MPa)					
EXPLC	84.2 (2.4) <sup>a,d</sup>	186.3 (2.9)	257.5 (1.3)	271.2 (9.8)	269.8 (2.7)	287.1 (6.9)
Fuji II LC	87.8 (2.3) <sup>a</sup>	120.9 (10)	125.7 (7.0)	141.5 (9.4)	149.8 (2.4)	150.6 (3.3)
	Modulus (GPa)					
EXPLC	4.67 (0.02)	7.32 (0.23)	8.82 (0.05)	9.06 (0.26)	9.04 (0.04)	9.18 (0.09)
Fuji II LC	3.62 (0.16)	5.33 (0.09)	5.40 (0.28)	5.64 (0.15)	5.74 (0.25)	5.34 (0.04)
	UCS <sup>c</sup> (MPa)					
EXPLC	210.9 (7.6)	277.9 (12)	323.3 (11.2)	320.1 (11.2)	322.1 (5.5)	345.7 (8.3)
Fuji II LC	181.5 (12)	212.7 (15)	219.1 (1.7)	208.6 (11)	218.0 (2.9)	213.5 (9.7)

<sup>a</sup>EXPLC: MW of the 6-arm PAA = 15 272 Daltons, filler = Fuji II LC, grafting ratio = 50%, P/W ratio = 75/25 and P/L ratio = 2.7; Fuji II LC: P/L ratio = 3.2 (per manufacturer's recommendation).

<sup>b</sup>Y<sub>S</sub> = CS at yield.

<sup>c</sup>UCS = Ultimate CS.

<sup>d</sup>Entries are mean values with standard deviations in parentheses and the mean values with the same superscript letter were not significantly different ( $p > 0.05$ ). Specimens were conditioned in distilled water at 37 °C prior to testing.

**Table 4.**

CS, DTS, FS and shrinkage comparisons between EXPLC and Fuji II LC cements.

Material <sup>a</sup>	CS (MPa)	DTS (MPa)	FS (MPa)	FT (MPa m <sup>-1/2</sup> )	Shrinkage (%)
EXPLC	323.3 (11)	61.7 (5.3)	103.5 (0.7)	1.45 (0.05)	0.9 (0.03)
Fuji II LC	219.1 (1.7)	34.9 (2.9)	53.0 (2.8)	0.91 (0.03)	4.7 (0.13)

<sup>a</sup>EXPLC: MW of the 6-arm PAA = 15 272 Daltons, filler = Fuji II LC, grafting ratio = 50%, P/W ratio = 75/25, = and P/L ratio = 2.7; Fuji II LC: P/L ratio = 3.2; specimens for CS, DTS, FS and FT tests were conditioned in distilled water at 37 °C for 1 week prior to testing. Specimens for shrinkage measurement were tested immediately after being light-cured.